Wideband Angle of Arrival Estimation Using the SAGE Algorithm

B. H. Fleury, D. Dahlhaus, R. Heddergott, M. Tschudin

Communication Technology Laboratory
Swiss Federal Institute of Technology Zurich
ETH-Zentrum, CH-8092 Zurich, Switzerland
{fleury,dahlhaus,ralf,tschudin}@nari.ee.ethz.ch

Abstract—**A new method for the high resolution of the electromagnetic field with respect to both the incidence direction and delay is presented. The underlying discrete propagation model relies on the assumption that a finite known number of transverse electromagnetic plane waves characterized by their complex amplitude, propagation delay, and azimuthal incidence direction are impinging in a neighborhood of the receiver position. A space-alternating generalized expectation-maximization (SAGE) algorithm is proposed to replace the high-dimensional optimization procedure necessary to compute the joint maximum-likelihood estimate of the waves' parameters by several separate maximization processes which can be performed sequentially. The resolution and the mean convergence rate of the scheme are evaluated by means of Monte-Carlo simulations considering discrete synthetic propagation environments. Finally, the applicability of the SAGE algorithm to real propagation environments is demonstrated.**

I. Introduction

In the last few years, issues concerning the spatial resolution of the received electromagnetic field have attracted a lot of attention in mobile communications [1], [2], [3], and [4]. There are many reasons for the continuously growing research activity on this topic. Accurate models for field prediction used by system providers to plan their networks necessitate powerful methods to identify the dominant propagation paths between the transmitter and the receiver as well as to compute the loss along these paths. The elaboration and the optimization of these methods require a sound knowledge of the main propagation mechanisms in the considered environment. This knowledge can solely be gained from experimental investigations of the channel by means of measurement techniques, possibly combined with a suitable data processing algorithm, which allow a resolution of the electromagnetic field with respect to (w.r.t.) both the propagation delay and the incidence direction. This issue is also of main concern to the designers of communications systems. Indeed, knowledge of the incidence direction allows to control the interference from other radio sources by means of employing sectorized or smart antennas. The latter adaptively match their pattern to the time-varying propagation conditions. Moreover, the ability of resolving the impinging waves according to their direction allows to exploit the inherent spatial diversity of the radio channel. Comprehensive experimental investigations [5], [6] have shown that these techniques will considerably increase the capacity of the third generation mobile radio systems. The high complexity of such systems exploiting either a part or all of the inherent channel diversity, i.e., the delay, the space, and the polarization diversity, precludes any complete theoretical analysis of their performance so that a resort to Monte Carlo simulations is unavoidable. However, this approach necessitates the elaboration of sophisticated channel models which describe the spread of the electromagnetic field w.r.t. both the delay and the incidence direction, rather than the channel impulse response, according to today's practice. Comprehensive experimental investigations by means of the aforementioned sounding techniques are also a prerequisite for the development of such simulation models which accurately reflect the propagation conditions in real environments.

The classical methods for incidence direction estimation are the Fourier [7] and beam-forming [8] techniques. Suboptimal methods have also been proposed such as the multiple signal classification (MUSIC), [9], [8], estimation of signal parameters via rotational invariance techniques (ESPRIT) [10] as well as the single-snapshot spatial separation (4xS) [11] and the virtual image array single snapshot (VIASS) algorithms [12]. In this paper, we propose a technique derived from the maximum-likelihood (ML) principle which allows for high-resolution of the electromagnetic field w.r.t. both the azimuthal incidence angle and the propagation delay. We use an extension of the expectation-maximization (EM) algorithm [13], [14], [15] referred to as the space-alternating generalized EM (SAGE) algorithm [16] to replace the high-dimensional optimization process necessary to compute the ML estimate of the waves' parameters by several separate, low-dimensional maximization procedures which are performed sequentially.

The paper is organized as follows. In Section II, we define the underlying propagation model. Section III is devoted to the derivation of the EM and SAGE algorithms. Finally, in Section IV the performance of the latter scheme is evaluated in both synthetic and real propagation environments.

II. Signal Model

The sounding signal consists of an infinite train of rectangular pulses modulated by a pseudo-noise (PN) sequence. It is worthwhile to write it as $\sqrt{E/T}u(t)$ with $u(t) = \sum_{i=-\infty}^{\infty} a(t - iT)$. Here, T denotes its period, E is its energy calculated over T, and $a(t) := \sum_{n=0}^{N-1} a_n \mathrm{rect}_{T_c}(t - nT_c)$ is the restriction of $u(t)$ to $[0, T)$. Furthermore, $\mathrm{rect}_{T_c}(t)$ is a unit rectangular pulse of

0-7803-3567-8/96/$5.00 © 1996 IEEE

duration T_c, while $N := T/T_c$ and $[a_0, \ldots, a_{N-1}] \in \{-1, +1\}^N$ denote the period and the restriction to $\{0, \ldots, N-1\}$, respectively, of the PN sequence.

The propagation model relies on the assumption that L (uniform transverse electromagnetic plane) waves are impinging in a neighborhood of the receiver location. The receiver consists of an array of M antennas or sensors and a processing unit which computes estimates of the waves' parameters from the sensors' outputs. The position of the sensors w.r.t. an arbitrary reference point O is described by the vectors $r_1 \ldots r_M \in \mathbb{R}^2$. Without loss of generality (w.l.o.g.) the reference point is assumed to coincide with the center of gravity of the array. The impulse response of the channel constituted by the transmitting antenna, the propagation medium, and the m-th sensor is given as

$$h_m(t) = \sum_{\ell=1}^{L} h_\ell \exp\{\jmath \tfrac{2\pi}{\lambda}\langle e(\phi_\ell), r_m\rangle\}\delta(t - (\tau_\ell - \tfrac{1}{c}\langle e(\phi_\ell), r_m\rangle)). \quad (1)$$

In this expression c and λ denote the velocity of light and the wavelength, respectively. Moreover, h_ℓ, ϕ_ℓ, and τ_ℓ are the complex weight, the incidence azimuthal angle and the propagation delay, respectively, of the ℓ-th impinging wave at location O with $\ell = 1 \ldots L$. Finally, $e(\phi)$ is the unit vector in $\mathbb{R}^2$ pointing towards the direction determined by ϕ, $\langle \cdot, \cdot \rangle$ stands for the scalar product and $\delta(\tau - \tau_0)$ denotes a Dirac impulse or measure at τ_0. The term $\frac{1}{c}\langle e(\phi_\ell), r_m\rangle$ in (1) expresses the difference between the propagation delays of the ℓ-th wave at the locations r_m and O. The subsequent investigations rely on the following model restrictions: (i) the term $\frac{1}{c}\langle e(\phi_\ell), r_m\rangle$ is sufficiently small to be neglected, and (ii) the spread of the impulse response (1) is smaller than T, i.e., $\max_{\ell,\ell'} |\tau_\ell - \tau_{\ell'}| < T$. W.l.o.g., the last condition can be replaced by $0 \le \tau_\ell < T$, $\ell = 1 \ldots L$.

The signals at the output of the sensors read

$$\begin{aligned} Y_m(t) &= \sqrt{E/T}u(t) * h_m(t) + N_m(t) \\ &= \sum_{\ell=1}^{L} \alpha_\ell \exp\{\jmath \tfrac{2\pi}{\lambda}\langle e(\phi_\ell), r_m\rangle\}u(t - \tau_\ell) \\ &\quad + N_m(t) \ , \ m = 1 \ldots M \end{aligned} \quad (2)$$

with $\alpha_\ell := \sqrt{E/T}h_\ell$ and $N_m(t) := N_{\Re,m}(t) + \jmath N_{\Im,m}(t)$ where $N_{\Re,m}(t)$ and $N_{\Im,m}(t)$ denote two independent zero-mean Gaussian white noise processes having a two-sided spectral density of height $N_0/2$. Using a vector notation allows to rewrite the M relations in (2) in a compact form according to

$$Y(t) = \sum_{\ell=1}^{L} c(\phi_\ell)\alpha_\ell u(t - \tau_\ell) + N(t), \quad (3)$$

where $Y(t) := [Y_1(t), \ldots, Y_M(t)]^{\mathrm{T}}$, $c(\phi) := \left[\exp\{\jmath \tfrac{2\pi}{\lambda}\langle e(\phi), r_1\rangle\}, \ldots, \exp\{\jmath \tfrac{2\pi}{\lambda}\langle e(\phi), r_M\rangle\}\right]^{\mathrm{T}}$ is the steering vector of the antenna array in the direction determined by ϕ, and $N(t) := [N_1(t), \ldots, N_M(t)]^{\mathrm{T}}$. Here, $(\cdot)^{\mathrm{T}}$ denotes transposition. The components of $N(t)$ are assumed to be independent. Henceforth, a process which exhibits all the features of $N(t)$ except that the real and imaginary part of its components may have a two-sided spectral density of different height, say $\beta N_0/2$ with $\beta > 0$, is referred to as a white Gaussian noise vector (WGNV) and will be denoted for short WGNV(β). In particular, $N(t)$ is a WGNV(1).

III. Parameter Estimation Using the SAGE Algorithm

A. Log-Likelihood Function

Defining

$$s(t; \theta_\ell) := c(\phi_\ell)\alpha_\ell u(t - \tau_\ell) \quad (4)$$

with $\theta_\ell := [\tau_\ell, \phi_\ell, \alpha_\ell]$, the identity (3) becomes

$$Y(t) = \sum_{\ell=1}^{L} s(t; \theta_\ell) + N(t). \quad (5)$$

From (5) the log-likelihood function of the parameter vector $\theta := [\theta_1, \ldots, \theta_L]$ given an observation $y(t)|_{[0,PT)}$ of $Y(t)$ over the interval $[0, PT)$ is of the form [17]

$$\Lambda(\theta; y(t)|_{[0,PT)})) = \frac{1}{N_0}\left[2\int_0^{PT} \Re\{s(t;\theta)^{\mathrm{H}} y(t)\}dt - \int_0^{PT} \|s(t;\theta)\|^2 dt\right] \quad (6)$$

where $s(t;\theta) := \sum_{\ell=1}^{L} s(t;\theta_\ell)$, $\Re\{\cdot\}$ is the real part of the function given as an argument, while $(\cdot)^{\mathrm{H}}$ and $\|\cdot\|$ denote the Hermitian operator and the Euclidean norm, respectively.

B. Maximum-Likelihood Estimation

A maximum-likelihood estimate (MLE) of θ based on the observation $y(t)|_{[0,PT)}$ is the value[1] of this vector which maximizes $\Lambda(\theta; y(t)|_{[0,PT)})$ [17], i.e.,

$$\hat{\theta}_{\mathrm{ML}}(y(t)|_{[0,PT)}) = \arg\max_{\theta} \Lambda(\theta; y(t)|_{[0,PT)}). \quad (7)$$

The maximization procedure to calculate $\hat{\theta}_{\mathrm{ML}}(y(t)|_{[0,PT)})$ is computationally prohibitive for large values of L because $\Lambda(\theta; y(t)|_{[0,PT)})$ is a non-linear function of θ and this procedure has to be performed in a high dimensional space, i.e., in $\mathbb{R}^{4L}$.

C. Expectation-Maximization Algorithm

The maximization of the likelihood function in (7) can be circumvented by resorting to the expectation-maximization (EM) algorithm [13], [14]. This scheme is derived within a conceptual framework where the received signal $Y(t)$ is regarded as the incomplete data which can be expressed as a function of a hypothetical complete but unobservable data. In the present application the incomplete data are selected according to $[X_1(t), \ldots, X_L(t)]$, where $X_\ell(t) := s(t; \theta_\ell) + N_\ell(t)$ with $N_\ell(t)$ denoting a WGNV(β_ℓ), $\ell = 1 \ldots L$. Moreover, $N_1(t) \ldots N_L(t)$ are independent and the positive constants $\beta_1 \ldots \beta_L$ satisfy $\sum_{\ell=1}^{L} \beta_\ell = 1$. The incomplete data $Y(t)$ can be written as a function of the complete data according to

$$Y(t) = \sum_{\ell=1}^{L} X_\ell(t) = \sum_{\ell=1}^{L} s(t; \theta_\ell) + \sum_{\ell=1}^{L} N_\ell(t). \quad (8)$$

Thus, the components of the complete data are obtained by decomposing the noise $N(t)$ into L independent parts and adding each of them to a corresponding

[1] For the sake of simplicity we assume that this value is unique.

received replica of the sounding signal. Due to the particular structure of the right-hand side of (8) the computation of the MLE $\hat{\theta}_{\mathrm{ML}}([x_1(t),\ldots,x_L(t)]|_{[0,PT)})$ of θ based on the observation $[x_1(t),\ldots,x_L(t)]|_{[0,PT)}$ actually requires L separate maximization procedures w.r.t. θ_ℓ, $\ell = 1\ldots L$, and consequently is less complex than the calculation of $\hat{\theta}_{\mathrm{ML}}(y(t)|_{[0,PT)})$ in (7). However, since the complete data are not observable, we consider instead of $\Lambda(\theta;[x_1(t),\ldots,x_L(t)]|_{[0,PT)})$ its conditional expectation given the observation $y(t)|_{[0,PT)}$ and assuming that $\theta = \theta'$:

$$U(\theta,\theta') := \mathbf{E}\left[\Lambda(\theta;[X_1(t),\ldots,X_L(t)]|_{[0,PT)}) \,\middle|\, y(t)|_{[0,PT)},\theta'\right]. \quad (9)$$

Using $U(\theta,\theta')$, an iterative algorithm can be built which, starting from an initial value $\hat{\theta}(0)$, generates a sequence $\{\hat{\theta}(\eta) : \eta \in \mathbb{N}_0\}$ as follows:

$$\hat{\theta}(\eta+1) = \arg\max_{\theta} U(\theta,\hat{\theta}(\eta)). \quad (10)$$

Here $\mathbb{N}_0 := \{0,1,2,\ldots\}$ is the set of non-negative integers. This scheme is a generalized EM algorithm [13] in the sense that $\{\Lambda(\hat{\theta}(\eta);y(t)|_{[0,PT)}) : \eta \in \mathbb{N}_0\}$ is non-decreasing. As a consequence $\{\hat{\theta}(\eta) : \eta \in \mathbb{N}_0\}$ may converge to (7). The computation of $\hat{\theta}(\eta+1)$ is made up of the so-called expectation (E)-step in which $U(\theta,\hat{\theta}(\eta))$ is calculated from (9) and the maximization (M)-step (10). Because of the particular choice of the complete data, the function $U(\theta,\theta')$ can be written as $U(\theta,\theta') = C + \sum_{\ell=1}^{L} U_\ell(\theta_\ell,\theta')$ where C is a constant which does not depend on θ. Thus, the M-step in (10) is performed by separately maximizing $U_\ell(\theta_\ell,\hat{\theta}(\eta))$ with respect to θ_ℓ for any $\ell = 1\ldots L$. In the EM algorithm the joint maximization procedure w.r.t. the $4L$-dimensional parameter vector θ in (7) is replaced by L separate maximization procedures w.r.t. the 4-dimensional parameter vectors θ_ℓ ($\ell = 1\ldots L$) which can be carried out in parallel.

The EM algorithm has been successfully applied to estimate the complex weights and the delays in a direct-sequence code division multiple access receiver which jointly performs multiuser detection and channel parameter estimation [15]. The EM algorithm described above is an extension of the former one to include the estimation of the incidence angle of the waves.

D. SAGE Algorithm

Due to the special structure of the function $U_\ell(\theta_\ell,\hat{\theta}(\eta))$ its maximization w.r.t. $\theta_\ell = [\tau_\ell,\phi_\ell,\alpha_\ell]$ actually reduces to the both next operations. First, $U_\ell(\theta_\ell,\hat{\theta}(\eta))$ is jointly maximized w.r.t. τ_ℓ and ϕ_ℓ while keeping α_ℓ fixed to obtain $\hat{\tau}_\ell(\eta+1)$ and $\hat{\phi}_\ell(\eta+1)$. Then, $\hat{\alpha}_\ell(\eta+1)$ is computed from a closed formula expressing it as a function of $\hat{\tau}_\ell(\eta+1)$ and $\hat{\phi}_\ell(\eta+1)$. To achieve an additional simplification of this optimization procedure it is desirable to replace the above joint maximization w.r.t. τ_ℓ and ϕ_ℓ by two separate maximizations w.r.t. these two parameters. However, the modified scheme should generate sequences of parameter estimates for which the likelihood function $\Lambda(\theta;y(t)|_{[0,PT)})$ is still increasing. This can be accomplished using an extension of the EM algorithm called space-alternating generalized EM (SAGE) algorithm [16]. The key idea behind the latter scheme consists in splitting up the parameters into several, possibly overlapping groups. Then, the EM algorithm is applied sequentially to update the parameters in each of these groups separately while keeping the other parameters constant. Associated to each group is a so-called admissible hidden data set. A data set is admissible for a given group of parameters if, and only if, it is complete in the sense of [13] provided the parameters not belonging to this group are known.

For the problem discussed here the parameter vector θ is split up into the following sequence of vectors: $\theta_{1,1},\theta_{1,2}\ldots\theta_{\ell,1},\theta_{\ell,2}\ldots\theta_{L,1},\theta_{L,2}$ where $\theta_{\ell,1} := [\tau_\ell,\alpha_\ell]$ and $\theta_{\ell,2} := [\phi_\ell,\alpha_\ell]$, $\ell = 1\ldots L$. Let us further define $\overline{\theta}_{\ell,j}$ and $\overline{\theta}_{\overline{\ell},j}$ to be the parameter vectors which result from deleting the components of $\theta_{\ell,j}$ in θ and θ_ℓ, respectively. For example, considering $j=1$, we have $\theta_{\ell,1} = [\tau_\ell,\alpha_\ell]$, $\overline{\theta}_{\ell,1} = [\theta_1,\ldots,\theta_{\ell-1},\phi_\ell,\theta_{\ell+1},\ldots,\theta_L]$, and $\overline{\theta}_{\overline{\ell},1} = \phi_\ell$. It can be shown that

$$X_{\ell,j}(t) := s(t;\theta_\ell) + N_{\ell,j}(t), \quad (11)$$

where $N_{\ell,j}(t)$ is a WGNV($\beta_{\ell,j}$) with $0 \le \beta_{\ell,j} \le 1$, is admissible for $\theta_{\ell,j}$. Notice that $\Lambda(\theta_{\ell,j},\overline{\theta}'_{\ell,j};x_{\ell,j}(t)|_{[0,PT)}) = \Lambda(\theta_{\ell,j},\overline{\theta}'_{\overline{\ell},j};x_{\ell,j}(t)|_{[0,PT)})$. The SAGE algorithm results from applying the same rationale which has been used for the derivation of the EM algorithm. Instead of (9) let us consider the conditional expectation

$$V_{\ell,j}(\theta_{\ell,j},\theta'_{\ell,j};\overline{\theta}'_{\ell,j}) := \mathbf{E}\left[\Lambda(\theta_{\ell,j},\overline{\theta}'_{\overline{\ell},j};X_{\ell,j}(t)|_{[0,PT)}) \,\middle|\, y(t)|_{[0,PT)},\theta'_{\ell,j},\overline{\theta}'_{\ell,j}\right]. \quad (12)$$

Notice that the two vectors $\theta'_{\ell,j},\overline{\theta}'_{\ell,j}$ arising in (12) can be concatenated to θ'. The $2L$ functions $V_{\ell,j}(\theta_{\ell,j},\theta'_{\ell,j};\overline{\theta}'_{\ell,j})$, $\ell = 1\ldots,L, j = 1,2$, can be applied as depicted in Fig. 1 to implement an algorithm which, starting from an initial value $\hat{\theta}(0)$ generates a sequence $\{\hat{\theta}(\eta) : \eta \in \mathbb{N}_0\}$. The admissibility of the hidden data guarantees that $\{\Lambda(\hat{\theta}(\eta);y(t)|_{[0,PT)}) : \eta \in \mathbb{N}_0\}$ is in this case also non-decreasing [16].

From (11) the likelihood function $\Lambda(\theta_{\ell,j},\overline{\theta}'_{\overline{\ell},j};x_{\ell,j}(t)|_{[0,PT)})$ is of the form

$$\Lambda(\theta_{\ell,j},\overline{\theta}'_{\overline{\ell},j};x_{\ell,j}(t)|_{[0,PT)}) = \frac{1}{\beta_{\ell,j}N_0}\left[2\int_0^{PT}\Re\{s(t;\theta_{\ell,j},\overline{\theta}'_{\overline{\ell},j})^{\mathrm{H}}x_{\ell,j}(t)\}dt - \int_0^{PT}\|s(t;\theta_{\ell,j},\overline{\theta}'_{\overline{\ell},j})\|^2dt\right].$$

If we take the conditional expectation of the right-hand side above given the observation $y(t)|_{[0,PT)}$ and assuming that $\theta = \theta'$ we obtain

$$V_{\ell,j}(\theta_{\ell,j},\theta'_{\ell,j};\overline{\theta}'_{\ell,j}) = \frac{1}{\beta_{\ell,j}N_0}\left[2\int_0^{PT}\Re\{s(t;\theta_{\ell,j},\overline{\theta}'_{\overline{\ell},j})^{\mathrm{H}}\hat{x}_{\ell,j}^{(\theta')}(t)\}dt - \int_0^{PT}\|s(t;\theta_{\ell,j},\overline{\theta}'_{\overline{\ell},j})\|^2dt\right], \quad (13)$$

where

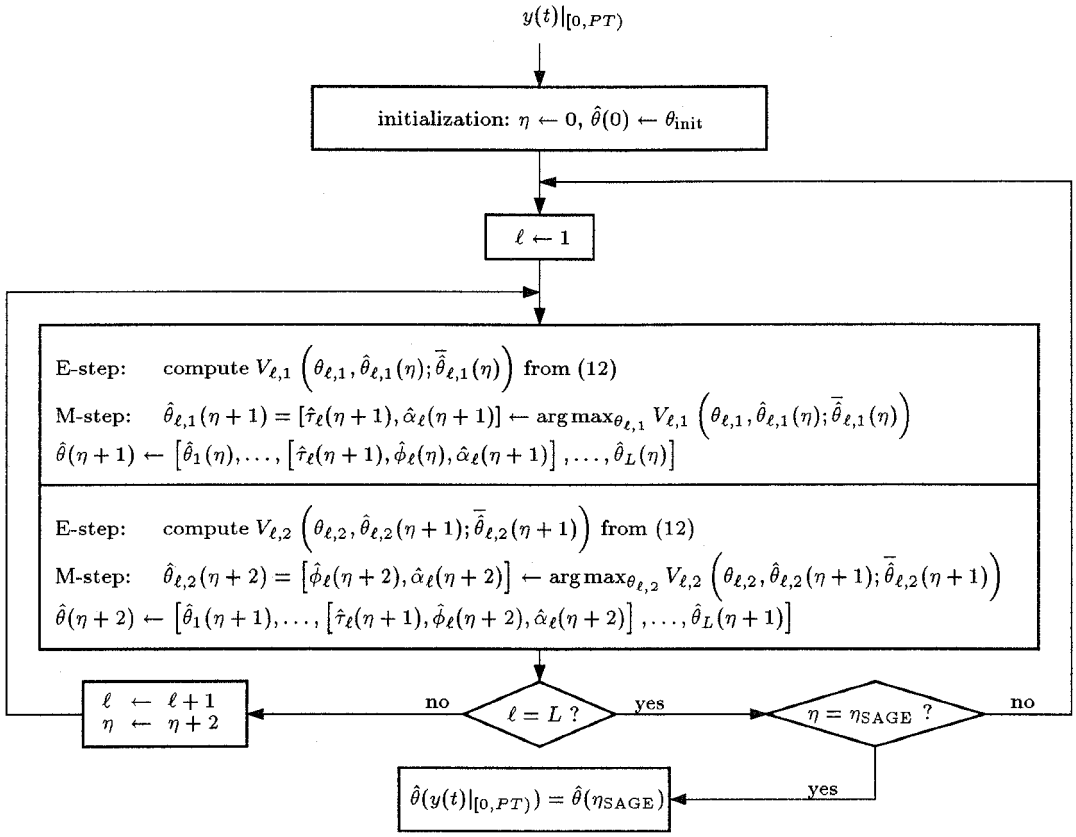

Figure 1: Basic implementation of the SAGE algorithm based on (12).

$$\hat{x}_{\ell,j}^{(\theta')}(t) := \mathbf{E}\left[X_{\ell,j}(t) \,\middle|\, y(t)|_{[0,PT)}, \theta'\right] = s(t;\theta'_\ell)|_{[0,PT)} + \beta_{\ell,j}\left[y(t)|_{[0,PT)} - \sum_{\ell'=1}^{L} s(t;\theta'_{\ell'})|_{[0,PT)}\right] \quad (14)$$

The function $\hat{x}_{\ell,j}^{(\theta')}(t)$ is an estimate of $X_{\ell,j}(t)|_{[0,PT)}$ based on the observation of $y(t)|_{[0,PT)}$ and assuming that $\theta = \theta'$. According to (14) it is obtained by adding an estimate of $N_{\ell,j}|_{[0,PT)}$ to the noiseless complete data $s(t;\theta'_\ell)|_{[0,PT)}$. Substituting (14) in (13) and making use of the definition (4) yield the following iteration equations (see Fig. 1) for the parameter estimates of the ℓ-th wave:

$\hat{\theta}_{\ell,1}$: - E-step:

Compute $\hat{x}_{\ell,1}^{(\hat{\theta}(\eta))}(t)$ from (14)

- M-step:

$$\hat{\tau}_\ell(\eta+1) = \arg\max_\tau \left| \int_0^{PT} u(t-\tau) c(\hat{\phi}_\ell(\eta))^{\mathrm{H}} \hat{x}_{\ell,1}^{(\hat{\theta}(\eta))}(t)\, dt \right| \quad (15)$$

$$\hat{\alpha}_\ell(\eta+1) = \frac{1}{MPT} \int_0^{PT} u(t-\hat{\tau}_\ell(\eta+1)) c(\hat{\phi}_\ell(\eta))^{\mathrm{H}} \hat{x}_{\ell,1}^{(\hat{\theta}(\eta))}(t)\, dt \quad (16)$$

$$\hat{\phi}_\ell(\eta+1) = \hat{\phi}_\ell(\eta)$$

$$\hat{\theta}_{\ell'}(\eta+1) = \hat{\theta}_{\ell'}(\eta)\,,\ \ell' \neq \ell$$

$\hat{\theta}_{\ell,2}$: - E-step:

Compute $\hat{x}_{\ell,2}^{(\hat{\theta}(\eta+1))}(t)$ from (14)

- M-step:

$$\hat{\phi}_\ell(\eta+2) = \arg\max_\phi \left| \int_0^{PT} u(t-\hat{\tau}_\ell(\eta+1)) c(\phi)^{\mathrm{H}} \hat{x}_{\ell,2}^{(\hat{\theta}(\eta+1))}(t)\, dt \right| \quad (17)$$

$$\hat{\alpha}_\ell(\eta+2) = \frac{1}{MPT} \cdot \int_0^{PT} u(t-\hat{\tau}_\ell(\eta+1)) c(\hat{\phi}_\ell(\eta+2))^{\mathrm{H}} \hat{x}_{\ell,2}^{(\hat{\theta}(\eta+1))}(t)\, dt \quad (18)$$

$$\hat{\tau}_\ell(\eta+2) = \hat{\tau}_\ell(\eta+1)$$

$$\hat{\theta}_{\ell'}(\eta+2) = \hat{\theta}_{\ell'}(\eta+1)\,,\ \ell' \neq \ell\,.$$

The integrals in (15) coincide with the periodic cross-correlation over $[0, PT)$ of the sounding signal and a function which results from summing up the suitably rotated components of the estimated hidden data $\hat{x}_{\ell,1}^{(\hat{\theta}(\eta))}(t)$. The rotation aims to compensate for the different phase shifts of the ℓ-th wave at the different sensors. Thus, $\hat{\tau}_\ell(\eta+1)$ is the time lag for which this cross-correlation function takes its maximum, while according to (16) $\hat{\alpha}_\ell(\eta+1)$ is equal to the value of this function at its maximum divided by M times the energy of $u(t)$ in the observation interval. Notice that $\hat{\phi}_\ell(\eta+2)$ in (17) is identical to the estimate which results from applying the

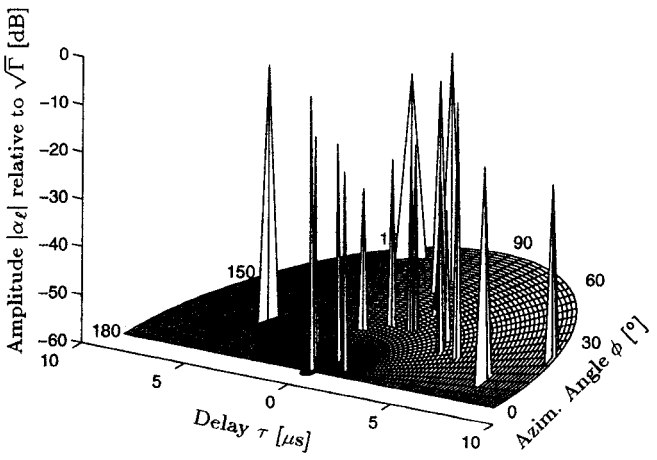

Figure 2: Application of the SAGE algorithm in a discrete synthetic propagation environment: absolute value of the channel direction-delay-spread function; Γ denotes the received power averaged over the M sensors.

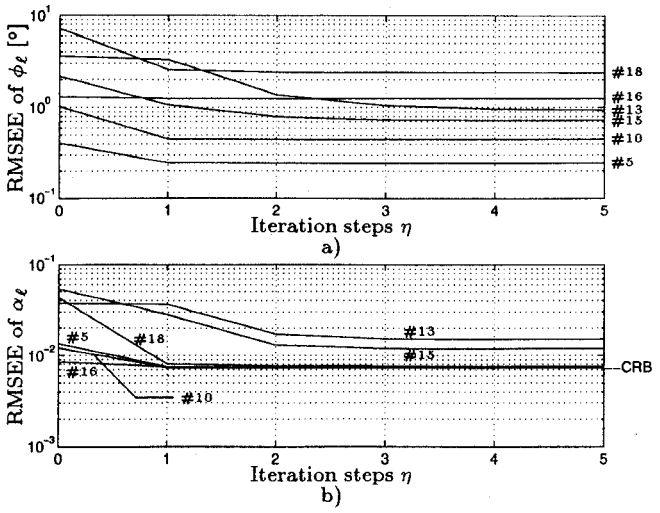

Figure 3: Application of the SAGE algorithm in a discrete synthetic propagation environment: behavior as a function of the number of iterations of the RMSEE for a) the azimuthal incidence angle and b) the complex amplitude of some selected waves.

beamforming method to the signal vector $\hat{x}_{\ell,2}^{(\hat{\theta}(\eta+1))}(t)$. Finally, the step in (18) corresponds to that in (16). The computation of the right-hand term in the four expressions above always relies on the latest update of the parameter values.

For the implementation of the SAGE algorithm we have followed the recommendation in [16] to set $\beta_{\ell,j} = 1$ for $\ell = 1 \ldots L$, $j = 1, 2$. This value minimizes the Fisher information matrix of the hidden-data which in turn results in an improved convergence rate and also in a larger increase of the likelihood function $\Lambda(\theta; y(t)|_{[0,PT)})$ at the early iteration steps. Moreover, this setting leads to a slightly reduction of the complexity of the SAGE-algorithm. Indeed, in this case $\hat{x}_{\ell,2}^{(\hat{\theta}(\eta+1))}(t) = \hat{x}_{\ell,1}^{(\hat{\theta}(\eta))}(t)$ in (15)-(18) because $\hat{x}_{\ell,j}^{(\theta')}(t)$ in (14) does not depend anymore on θ'_ℓ.

We propose the following initialization of the SAGE algorithm. In the absence of any a priori knowledge of the channel parameters the sensor outputs are incoherently combined to provide the initial delay estimates. Thus, $\hat{\tau}_1(0), \ldots, \hat{\tau}_L(0)$ are the values of τ for which the function $\sum_{m=1}^{M} \left| \int_0^{PT} u(t-\tau) y_m(t)\, dt \right|^2$ takes its L largest local maxima. Then, for each $\ell = 1 \ldots L$,

$$\hat{\phi}_\ell(0) = \arg\max_{\phi} \left| \int_0^{PT} u(t - \hat{\tau}_\ell(0)) c(\phi)^{\mathrm{H}} y(t)\, dt \right|,$$

$$\hat{\alpha}_\ell(0) = \frac{1}{MPT} \int_0^{PT} u(t - \hat{\tau}_\ell(0)) c(\hat{\phi}_\ell(0))^{\mathrm{H}} y(t)\, dt.$$

The initial settings for the incidence direction and the factors α_ℓ, $\ell = 1 \ldots L$, are obtained in a way similar to (17) and (18) based on $y(t)|_{[0,PT)}$ instead of (14).

IV. Performance Evaluation and Application of the SAGE Algorithm

The performance of the SAGE algorithm applied to process the output signals of a linear array antenna has been evaluated in synthetically generated propagation channels by means of Monte-Carlo simulations. The considered linear antenna array consists of $M = 5$ equidistant sensors with $\lambda/2$ separation. The modulating PN-sequence has a period $N = 127$. The chip duration is chosen such that the period of the sounding signal is 10 μs, i.e., $T_c = 78.7$ ns. The discretization steps of the SAGE algorithm are $T_c/10 = 7.87$ ns and 0.5 ° (degree) for the delay and the azimuthal angle, respectively. The root-mean-square estimation error (RMSEE) for the waves' parameters has been investigated considering a fixed, synthetic propagation environment characterized by the direction-delay-spread function whose absolute value is shown in Fig. 2. Note the ambiguity in the estimation of ϕ which results from using a linear antenna array. The specular impinging waves have been generated using a COST 207 bad urban (BU) channel model [18] which has been modified to embody the azimuthal incidence angles. The number of waves is 20. The waves' angles and delays have been randomly and independently chosen according to a uniform distribution over [0, 10] μs and [0,360) °, respectively. The real and imaginary parts of the factors α_ℓ, $\ell = 1 \ldots L$, are realizations of independent zero-mean Gaussian random variables with equal variance proportional to the value of the power-delay profile of the BU channel at the corresponding delay. The SNR equals 20 dB, which corresponds to a realistic value in a measurement scenario.

The waves with a relative SNR higher than -19 dB

Path number ℓ	$\alpha_\ell/\sqrt{\Gamma}$ [dB]	Delay τ_ℓ [μs]	Azimuthal angle ϕ_ℓ [°]
5	-14.42	0.98	65.0
10	-20.99	3.78	69.5
13	-22.34	3.54	69.0
15	-24.89	3.50	82.0
16	-30.45	2.96	98.0
18	-33.11	4.63	49.5

Table 1: Characteristics of the selected waves.

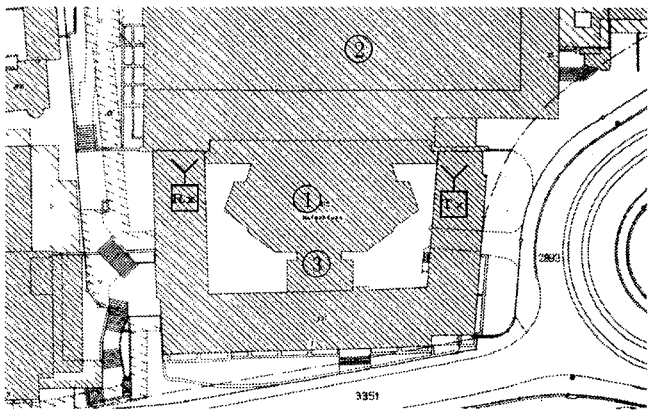

Figure 4: Application of the SAGE algorithm in a real propagation environment: map of the surroundings with receiver (Rx) and transmitter (Tx) location.

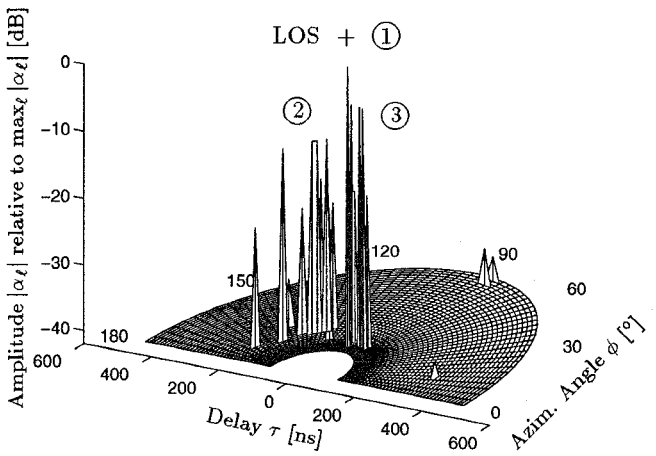

Figure 5: Application of the SAGE algorithm in a real propagation environment: absolute value of the estimated direction-delay spread function.

have always been correctly detected by the SAGE algorithm. The weaker ones were occasionally missed. The relative frequency of missing increases for decreasing relative SNR and also depends on the incidence direction, due to the non-isotropic pattern of the linear array. Provided that the waves are correctly detected, the mean convergence of the delay estimates is essentially achieved within one iteration. Then, the RMSEE stabilizes at a value smaller than the delay resolution $T_c/10$. The behavior of the RMSEE for the azimuthal angle of some selected waves (see Table 1) is depicted as a function of the number of iteration steps in Fig. 3.a. Except for waves #13 and #15, mean convergence is also essentially achieved within one iteration step. Then, the RMSEE reaches a value which depends on the strength of the corresponding wave and its incident direction because of the non-isotropic pattern of the array. The slow mean convergence of the angle estimate of waves #13 and #15 indicates that the scheme has difficulty in resolving them. The initial angle estimates provided by the beamforming method are in general already close to the true values when the waves are well resolvable either in direction or in delay. From Fig. 3.b we conclude that mean convergence for the complex attenuation estimates is also essentially achieved within two steps provided the waves are resolvable. In this case, the RMSEE stabilizes at a value close to the Cramér-Rao lower bound (CRB) [17] obtained from considering each wave alone. Otherwise, the RMSEE converges more slowly to a value larger than this bound (see waves #13 and #15).

The SAGE algorithm has been applied to resolve the electromagnetic field at 1.98 GHz in a real environment characteristic of a picocell (cf. Fig. 4). A line-of-sight (LOS) path exists between the transmitter (Tx) and the receiver (Rx) which are located 45 m apart. Indeed, as cannot be recognized from Fig. 4, the rooftop of building ① is lower than the direct path between both antennas. The output signals of a hypothetical linear array consisting of $M = 19$ equidistant sensors with 0.4λ separation are identified with the channel impulse response measured at the corresponding locations. The modulating PN-sequence has a period of $N = 255$ and the chip duration is $T_c = 10$ ns. The channel parameter estimates are obtained after 60 iterations of the SAGE algorithm. The selected discretization steps for the delays and azimuthal angles are 1 ns and 0.5 °, respectively. The absolute value of the estimated direction-delay spread function is depicted in Fig. 5. We can identify three main clusters. The first one is contributed by the direct wave (LOS path) as well as some slightly delayed waves which result from reflections on the roof of building ① . The second cluster which is due to reflection/scattering from the large building ② exhibits a substantial spread in space and also to some extent in delay. The last one is contributed by the superstructure ③ . This application example demonstrates that the SAGE algorithm whose derivation actually relies on a discrete propagation model is nevertheless able to deal with diffuse scattering, a situation quite often encountered in mobile radio.

V. Conclusions

A SAGE algorithm has been proposed in combination with a linear array to achieve a high-resolution of the electromagnetic field according to both the azimuthal incidence angle and the propagation delay. In this scheme, the cumbersome high-dimensional optimization process required to compute the ML estimate of the channel parameters is replaced by many separate optimization procedures which are performed sequentially. Extensive Monte-Carlo simulations show that the algorithm rapidly converges in synthetic discrete propagation environments provided that the waves are well resolvable with respect to their delay or incidence direction. Otherwise, the convergence is slower. Moreover, the SAGE algorithm has been successfully applied in a real propagation environment. The results point out the need for a theoretical treatment concerning the resolution ability of the scheme and its behavior when components exist in the direction-delay spread function which are due to diffuse scattering.

References

[1] S. Anderson, M. Millnert, M. Viberg, and B. Wahlberg, "An adaptive array for mobile communication systems," *IEEE Transactions on Vehicular Technology*, vol. 40, pp. 230–236, Feb. 1991.

[2] J. Fuhl and A. Molisch, "Space domain equalisation for second and third generation mobile radio systems," in *Proc. of the 2nd ITG Fachtagung Mobile Kommunikation '95*, vol. 135, (Neu-Ulm, Germany), pp. 85–92, Sept. 1995.

[3] C. Farsakh, M. Haardt, J. Nossek, and K. Pensel, "Adaptive antenna arrays in mobile radio systems," in *Proc. of the 2nd ITG Fachtagung Mobile Kommunikation '95*, vol. 135, (Neu-Ulm, Germany), pp. 101–108, Sept. 1995.

[4] S. Y. Miller and S. C. Schwartz, "Integrated spatial-temporal detectors for asynchronous Gaussian multiple-access channels," *IEEE Trans. Commun.*, vol. COM-43, pp. 396–411, Feb./Mar./Apr. 1995.

[5] P. C. Eggers, G. F. Pedersen, and K. Olesen, *Multisensor Propagation.* No. Rep. R2108/AUC/WP3.1/DS/I/046/b1, RACE Technology in Smart Antennas for Universal Advanced Mobile Infrastructure (TSUNAMI), Aug. 1994.

[6] P. C. Eggers, "Einfluss der Geländestreuung auf die Strahlungseigenschaften von Basisstationsrichtantennen für Mobilfunksysteme," *Nachrichtentech., Elektron., ne SCIENCE*, vol. 45, no. 4, pp. 57–62, 1995.

[7] S. Haykin and J. H. Justice, *Array Signal Processing.* Prentice Hall, Inc., Englewood Cliffs, New Jersy, 1985.

[8] S. U. Pillai, *Array Signal Processing.* Springer Verlag, 1989.

[9] R. O. Schmidt, "Multiple emitter location and signal parameter estimation," *IEEE Trans. Antennas and Propagation*, vol. AP-34, pp. 276–280, Mar. 1986.

[10] B. Ottersten and T. Kailath, "Direction of arrival estimation for wide-band signals using the ESPRIT algorithm," *IEEE Trans. Acoust., Speech, Signal Processing*, vol. 38, no. 2, pp. 317–327, 1990.

[11] M. E. Ali-Hackl, M. Haardt, and J. Nossek, "Single snapshot spatial separation (4xS) of wavefronts via antenna arrays," *Proc. 8th Aachener Kolloqium Signaltheorie, Aachen*, pp. 369–372, 1994.

[12] J. Fuhl, "Virtual-image-array-single-snapshot (VIASS) algorithm for direction-of-arrival estimation of coherent signals," Tech. Rep. COST 231 TD(95) 023, COST 231, Jan. 1995.

[13] A. P. Dempster, N. M. Laird, and D. B. Rubin, "Maximum likelihood from incomplete data via the EM algorithm," *J. Royal Statist. Soc., Ser. B*, vol. 39, no. 1, pp. 1–38, 1977.

[14] M. Feder and E. Weinstein, "Parameter estimation of superimposed signals using the EM algorithm," *IEEE Trans. Acoust., Speech, Signal Processing*, vol. ASSP-36, pp. 477–489, Apr. 1988.

[15] D. Dahlhaus, B. H. Fleury, and A. Radović, "A sequential algorithm for joint parameter estimation and multiuser detection in DS/CDMA systems with multipath propagation," *Wireless Personal Communications Journal*, To appear.

[16] J. A. Fessler and A. O. Hero, "Space-alternating generalized expectation-maximization algorithm," *IEEE Trans. on Signal Processing*, vol. 42, pp. 2664–2677, Oct. 1994.

[17] H. V. Poor, *An Introduction to Signal Detection and Estimation.* New York, NY: Springer-Verlag, 1988.

[18] COST 207 Management Committee, *COST 207: Digital Land Mobile Radio Communications (Final Report).* Commission of the European Communities, 1989.